Enhancing Compressed Sensing Photoacoustic Tomography by Simultaneous Motion Estimation

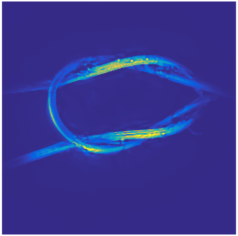 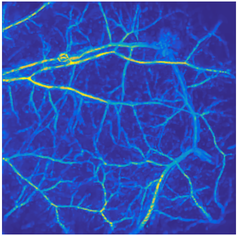 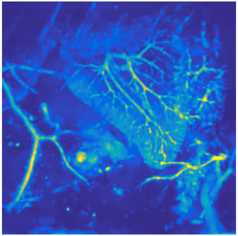

Felix Lucka
University College London
f.lucka@ulc.ac.uk

joint with:
Simon Arridge, Paul Beard, Marta Betcke,
Ben Cox, Nam Huynh & Edward Zhang

cmic
Centre for Medical Image Computing

Shape, Images and Optimization
Münster, Mar 2, 2017.

UCL CENTRE FOR INVERSE PROBLEMS

Optical Part

optical absorption coefficient: μ_a

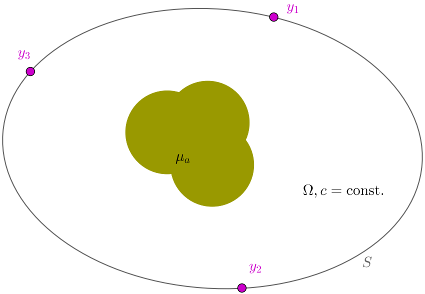

Acoustic Part

Basics of Photoacoustic Tomography (PAT)

Optical Part

optical absorption coefficient: μ_a

pulsed laser excitation: Φ

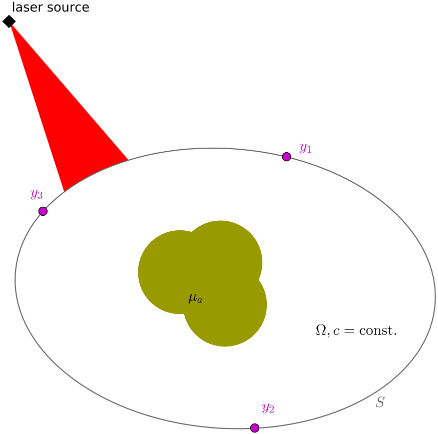

Acoustic Part

Optical Part

optical absorption coefficient: μ_a

pulsed laser excitation: Φ

thermalization by chromophores: $H = \mu_a \Phi$

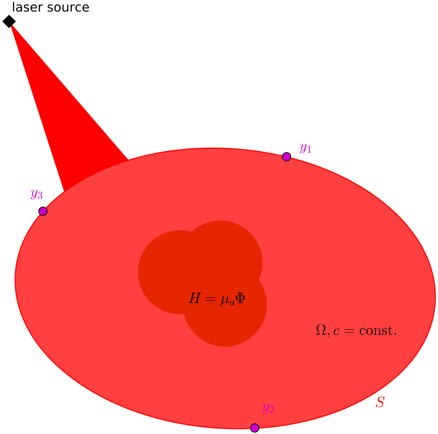

Acoustic Part

Basics of Photoacoustic Tomography (PAT)

Optical Part

optical absorption coefficient: μ_a

pulsed laser excitation: Φ

thermalization by chromophores: $H = \mu_a \Phi$

Acoustic Part

local pressure increase: $p_0 = \Gamma H$

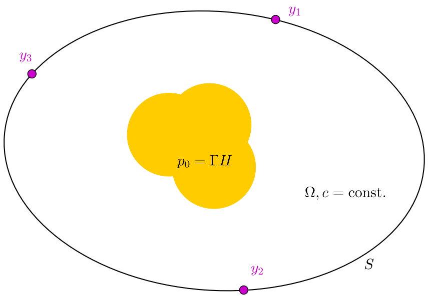

Optical Part

optical absorption coefficient: μ_a

pulsed laser excitation: Φ

thermalization by chromophores: $H = \mu_a \Phi$

Acoustic Part

local pressure increase: $p_0 = \Gamma H$

elastic wave propagation:

$$\Delta p - \frac{1}{c^2}\frac{\partial^2 p}{\partial^2 t} = 0$$

$$p|_{t=0} = p_0, \quad \frac{\partial p}{\partial t}|_{t=0} = 0$$

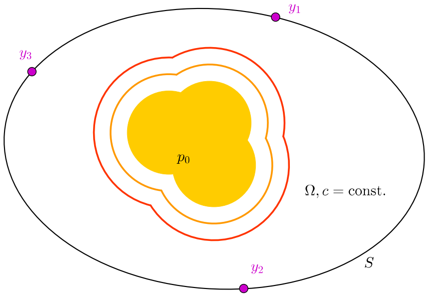

Basics of Photoacoustic Tomography (PAT)

Optical Part

optical absorption coefficient: μ_a

pulsed laser excitation: Φ

thermalization by chromophores: $H = \mu_a \Phi$

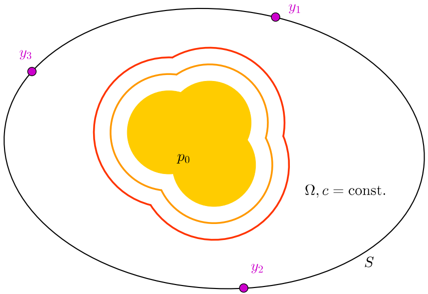

Acoustic Part

local pressure increase: $p_0 = \Gamma H$

elastic wave propagation:

$$\Delta p - \frac{1}{c^2}\frac{\partial^2 p}{\partial^2 t} = 0$$

$$p|_{t=0} = p_0, \quad \frac{\partial p}{\partial t}|_{t=0} = 0$$

measurement of pressure time courses:

$$f_i(t) = p(y_i, t)$$

Optical Part

optical absorption coefficient: μ_a

pulsed laser excitation: Φ

thermalization by chromophores: $H = \mu_a \Phi$

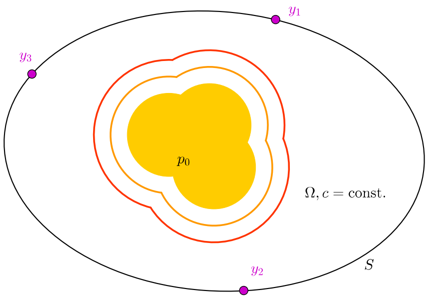

Acoustic Part

local pressure increase: $p_0 = \Gamma H$

elastic wave propagation:

$$\Delta p - \frac{1}{c^2}\frac{\partial^2 p}{\partial^2 t} = 0$$

$$p|_{t=0} = p_0, \quad \frac{\partial p}{\partial t}|_{t=0} = 0$$

measurement of pressure time courses:

$$f_i(t) = p(y_i, t)$$

Photoacoustic effect

- coupling of optical and acoustic modalities.
- "hybrid imaging"
- high optical contrast can be read by high-resolution ultrasound.

Optical Part

optical absorption coefficient: μ_a

pulsed laser excitation: Φ

thermalization by chromophores: $H = \mu_a \Phi$

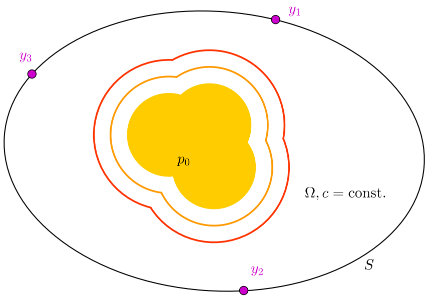

Acoustic Part

local pressure increase: $p_0 = \Gamma H$

elastic wave propagation:

$$\Delta p - \frac{1}{c^2}\frac{\partial^2 p}{\partial^2 t} = 0$$

$$p|_{t=0} = p_0, \quad \frac{\partial p}{\partial t}|_{t=0} = 0$$

measurement of pressure time courses:

$$f_i(t) = p(y_i, t)$$

Inverse problems:

! optical inversion (μ_a) from boundary data: severely ill-posed.

Basics of Photoacoustic Tomography (PAT)

Optical Part

optical absorption coefficient: μ_a

pulsed laser excitation: Φ

thermalization by chromophores: $H = \mu_a \Phi$

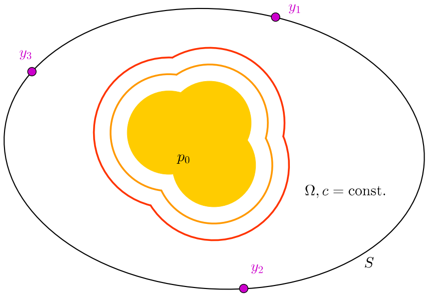

Acoustic Part

local pressure increase: $p_0 = \Gamma H$

elastic wave propagation:

$$\Delta p - \frac{1}{c^2} \frac{\partial^2 p}{\partial^2 t} = 0$$

$$p|_{t=0} = p_0, \quad \frac{\partial p}{\partial t}|_{t=0} = 0$$

measurement of pressure time courses:

$$f_i(t) = p(y_i, t)$$

Inverse problems:

! optical inversion (μ_a) from boundary data: severely ill-posed.

✓ acoustic inversion (p_0) from boundary data: moderately ill-posed.

✓ optical inversion (μ_a) from internal data: moderately ill-posed.

Photoacoustic Imaging: Applications

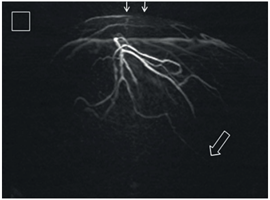

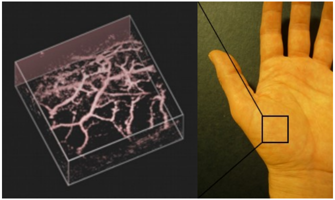

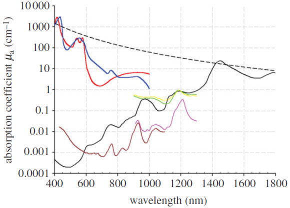

- Light-absorbing structures in soft tissue.
- High contrast between blood and water/lipid.
- Gap between oxygenated and deoxygenated blood.
- Different wavelengths allow quantitative spectroscopic examinations.
- Use of contrast agents for molecular imaging.
- Extremely promising future imaging technique!

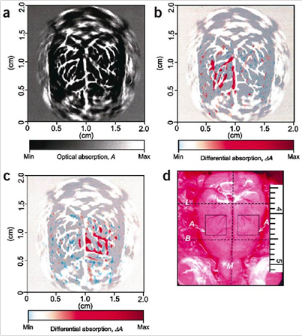

sources: **Paul Beard, 2011**. *Biomedical photoacoustic imaging, Interface Focus.* Wikimedia Commons

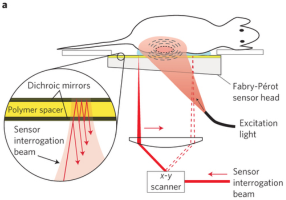

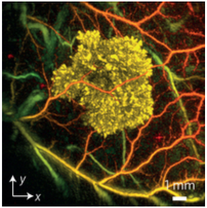

Fabry Pérot (FB) interferometer:

- ✓ High spatial resolution
- ! Nyquist sampling leads to low temporal resolution

$\rightsquigarrow$ Beat Nyquist for sparse targets by incoherent sampling of each frame/wavelength i ("compressed sensing"):

$$f_i^c = C_i f_i = C_i(Ap_i + \varepsilon_i), \qquad i = 1, \ldots, T$$

Image reconstruction:

$f_i^c \longrightarrow f_i$, $f_i \longrightarrow p_i$ by standard method.

$f_i^c \longrightarrow p_i$: standard or new method?

$F^c \longrightarrow P$: Full spatio-temporal method.

PAT Reconstruction & Numerical Wave Propagation

Variational regularization:

$$\hat{p} = \underset{p \geqslant 0}{\operatorname{argmin}} \left\{ \tfrac{1}{2} \| CAp - f^c \|_2^2 + \lambda \mathcal{J}(p) \right\}$$

! Iterative first-order methods require implementation of A and A^*.

✓ k-space pseudospectral time domain method for 3D wave propagation:

B. Treeby and B. Cox, 2010. *k-Wave: MATLAB toolbox for the simulation and reconstruction of photoacoustic wave fields*, Journal of Biomedical Optics.

✓ Derivation and discretization of adjoint PAT operator A^*:

Arridge, Betcke, Cox, L, Treeby, 2016. *On the Adjoint Operator in Photoacoustic Tomography*, Inverse Problems 32(11).

$$\hat{p}_i = \underset{p \geqslant 0}{\operatorname{argmin}} \left\{ \tfrac{1}{2} \| C_i A p - f_i^c \|_2^2 + \lambda \mathcal{J}(p) \right\}$$

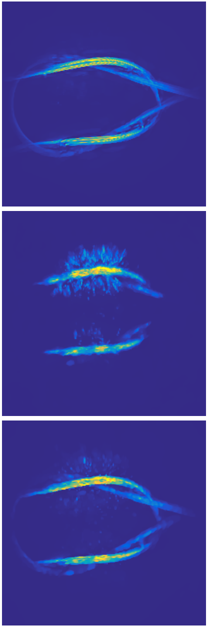

- ✓ combination of compressed sensing and sparsity-constrained image reconstruction
- ✓ generic total variation (TV) regularization enhanced by Bregman iterations
- ✓ extensive evaluation with realistic numerical phantom, experimental and *in-vivo* data
- ✓ significant acceleration with minor loss of quality.
- ! frame-by-frame reconstruction, only.

Arridge, Beard, Betcke, Cox, Huynh, L, Ogunlade, Zhang, 2016. *Accelerated High-Resolution Photoacoustic Tomography via Compressed Sensing*, *Physics in Medicine and Biology* 61(24).

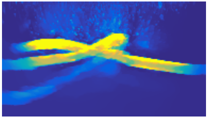

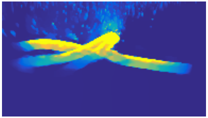

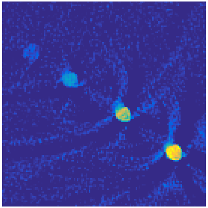

Continuous data acquisition

$\Longrightarrow$ tradeoff between spatial and temporal resolution.

Different dynamic models:

- Structured Low-Rank (functional imaging with static anatomies/QPAT).
- Tracer uptake/wash-in models.
- Perfusion models.
- Needle guidance
- Joint image reconstruction and motion estimation.

Spatio-Temporal Reconstruction: 4D PAT

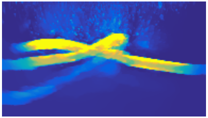

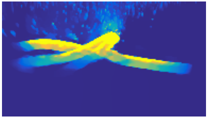

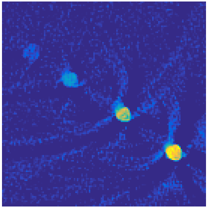

Continuous data acquisition

$\Longrightarrow$ tradeoff between spatial and temporal resolution.

Different dynamic models:

- Structured Low-Rank (functional imaging with static anatomies/QPAT).
- Tracer uptake/wash-in models.
- Perfusion models.
- Needle guidance
- Joint image reconstruction and motion estimation.

$$\hat{p}_i = \underset{p \geqslant 0}{\operatorname{argmin}} \left\{ \tfrac{1}{2} \| C_i A p - f_i^c \|_2^2 + \lambda TV(p) \right\}, \qquad \forall\ t = 1, \ldots, T$$

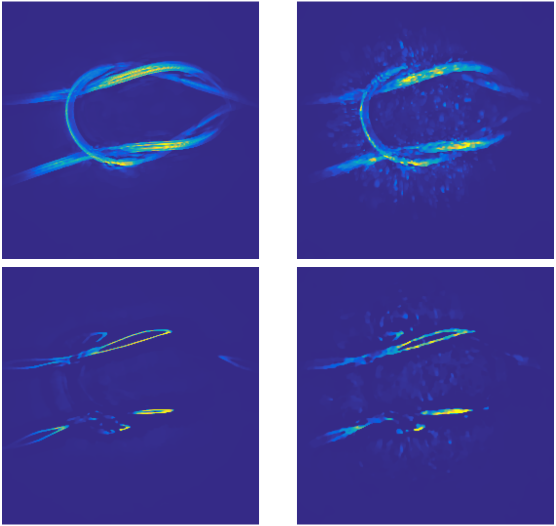

full data

sub-sampled data (16x)

Spatio-Temporal Regularization

Non-parametric spatio-temporal regularization: Find $P \in \mathbb{R}^{N \times T}$ as

$$\hat{P} = \underset{P \geqslant 0}{\operatorname{argmin}} \left\{ \sum_i^T \frac{1}{2} \| C_i A \, p_i - f_i^c \|_2^2 + \lambda \mathcal{R}(P) \right\},$$

Lot's of possibilities, here: Implicit model formulated as joint image and motion estimation:

$$(\hat{P}, \hat{V}) = \underset{P \geqslant 0, V}{\operatorname{argmin}} \left\{ \sum_i^T \frac{1}{2} \| C_i A \, p_i - f_i^c \|_2^2 + \alpha \mathcal{J}(p_i) + \beta \mathcal{H}(v_i) + \gamma \mathcal{S}(P, V) \right\}$$

$\mathcal{S}(P, V)$ enforces motion PDE, e.g., optical flow equation:

$$\partial_t p(x, t) + (\nabla_x p(x, t)) \, v(x, t) = 0$$

Burger, Dirks, Schönlieb, 2016. *A Variational Model for Joint Motion Estimation and Image Reconstruction*, arXiv:1607.03255.

Example: TV-TV-Lp Regularization

$$\partial_t p(x,t) + (\nabla_x p(x,t))\, v(x,t) = 0$$

$\rightsquigarrow$ discretize and penalize deviation:

$$(\hat{P}, \hat{V}) = \operatorname*{argmin}_{P \geqslant 0, V} \left\{ \sum_i^T \frac{1}{2} \| C_i A\, p_i - f_i^c \|_2^2 \right.$$

$$\left. + \alpha\, TV(p_i) + \beta\, TV(v_i) + \frac{\gamma}{p} \| (p_{i+1} - p_i) + (\nabla p_i) \cdot v_i \|_p^p \right\}$$

proximal-gradient-type scheme:

$$P^{k+1} = \mathbf{prox}_{\nu \mathcal{R}} \left(P^k - \nu A^T C^T \left(CAP^k - F^c \right) \right)$$

$$\mathbf{prox}_{\nu \mathcal{R}}(P) = \operatorname*{argmin}_{Q \geqslant 0} \left\{ \frac{1}{2} \| Q - P \|_2^2 + \nu \mathcal{R}(Q) \right\}$$

$$= \operatorname*{argmin}_{Q \geqslant 0} \left\{ \min_V \sum_i^T \frac{1}{2} \| q_i - p_i \|_2^2 \right.$$

$$\left. + \nu\alpha\, TV(q_i) + \nu\beta\, TV(v_i) + \frac{\nu\gamma}{p} \| (q_{i+1} - q_i) + (\nabla q_i) \cdot v_i \|_p^p \right\}$$

For $p \geqslant 1$, TV-TV-Lp denoising is a biconvex optimization problem:

$$\min_{Q \geqslant 0, V} S(Q, V) := \min_{Q \geqslant 0, V} \sum_{i}^{T} \frac{1}{2} \|q_i - p_i\|_2^2 + \nu\alpha TV(q_i) + \nu\beta TV(v_i) + \frac{\nu\gamma}{p} \|(q_{i+1} - q_i) + (\nabla q_i) \cdot v_i\|_p^p$$

Alternating optimization:

$$Q^{k+1} = \underset{Q}{\operatorname{argmin}}\, S(Q, V^k) \qquad \text{(TV-transport constr. denoising)}$$

$$V^{k+1} = \underset{V}{\operatorname{argmin}}\, S(Q^{k+1}, V) \qquad \text{(TV constr. optical flow estimation)}$$

! Both problems are convex but non-smooth.

! Need to ensure energy decrease.

Alternating optimization:

$$Q^{k+1} = \underset{Q}{\operatorname{argmin}}\, S(Q, V^k) \qquad \text{(TV-transport constr. denoising)}$$

$$V^{k+1} = \underset{V}{\operatorname{argmin}}\, S(Q^{k+1}, V) \qquad \text{(TV constr. optical flow estimation)}$$

Primal-dual hybrid gradient for both: Too slow convergence in 3D.

Alternating directions method of multipliers (ADMM):

- ! More difficult to parameterize (to ensure monotone energy).
- ! Badly conditioned, large-scale least-squares problems.
- ! Crucial: Choice of iterative solver, preconditioning and stop criterion.
- ✓ Overrelaxed ADMM with step size adaptation and CG solver for Q.
- ✓ Overrelaxed ADMM with AMG-CG solver for V (frame-by-frame).
- ✓ Warm-start wherever possible.

Detailed evaluation in process!

A 2D Example: Frame-by-Frame Least Squares

$$\hat{p}_i = \underset{p \geqslant 0}{\operatorname{argmin}} \left\{ \| C_i A p - f_i^c \|_2^2 \right\} \quad \forall \; i = 1, \ldots, K$$

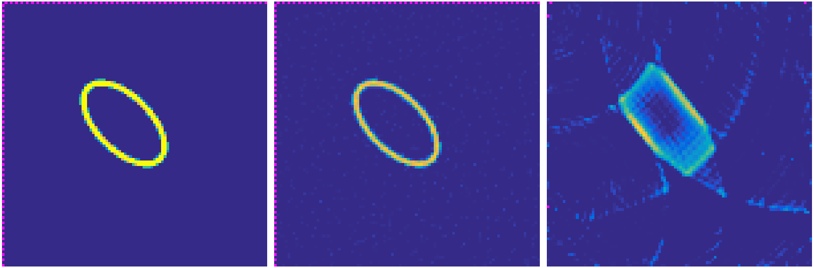

phantom | full data | sub-sampled (25x)

$$\hat{p}_i = \underset{p \geqslant 0}{\operatorname{argmin}} \left\{ \| C_i A p - f_i^c \|_2^2 + \lambda TV(p) \right\} \quad \forall\, i = 1, \ldots, K$$

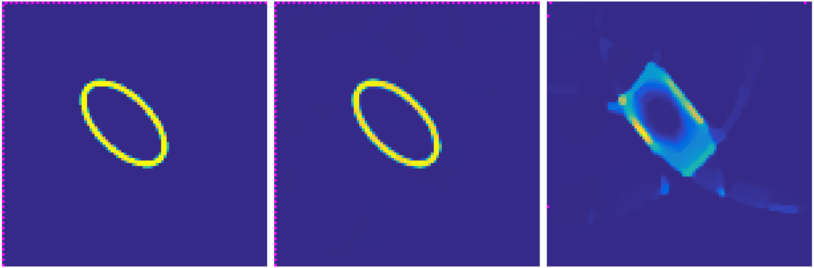

phantom | full data | sub-sampled (25x)

$$\left(\hat{P}, \hat{V}\right) = \underset{P \geqslant 0, V}{\operatorname{argmin}} \left\{ \frac{1}{2} \sum_{i}^{T} \| C_i A\, p_i - f_i^c \|_2^2 \right.$$
$$\left. + \alpha TV(p_i) + \beta TV(v_i) + \gamma \| (p_{i+1} - p_i) + \nabla p_i \cdot v_i \|_2^2 \right\}$$

$\alpha = \beta = \lambda_{TV}$, $\gamma = 1$.

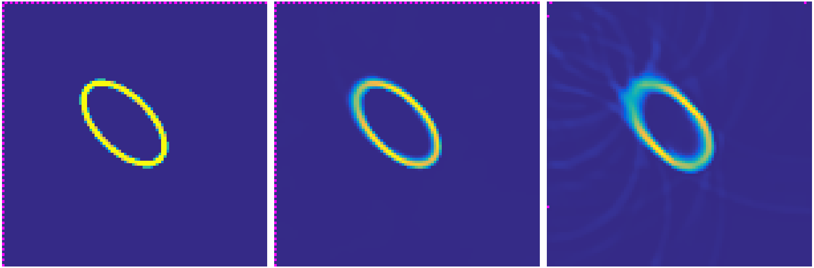

phantom | full data | sub-sampled (25x)

A 2D Example: TV-TV-L2

$$\left(\hat{P}, \hat{V}\right) = \underset{P \geqslant 0, V}{\operatorname{argmin}} \left\{ \frac{1}{2} \sum_{i}^{T} \| C_i A\, p_i - f_i^c \|_2^2 \right.$$
$$\left. + \alpha\, TV(p_i) + \beta\, TV(v_i) + \gamma \| (p_{i+1} - p_i) + \nabla p_i \cdot v_i \|_2^2 \right\}$$

$\alpha = \beta = \lambda_{TV}$, $\gamma = 0.1$.

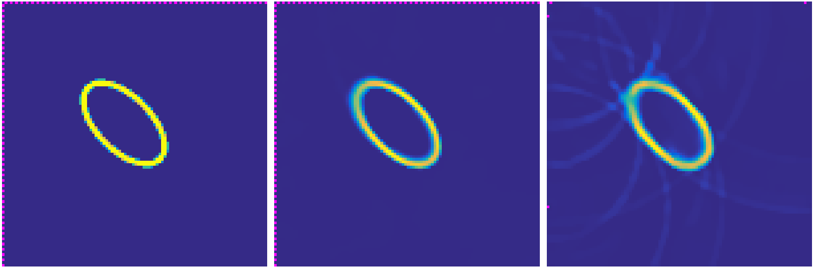

phantom | full data | sub-sampled (25x)

Artificially Sub-Sampled 3D Stop-Motion Data

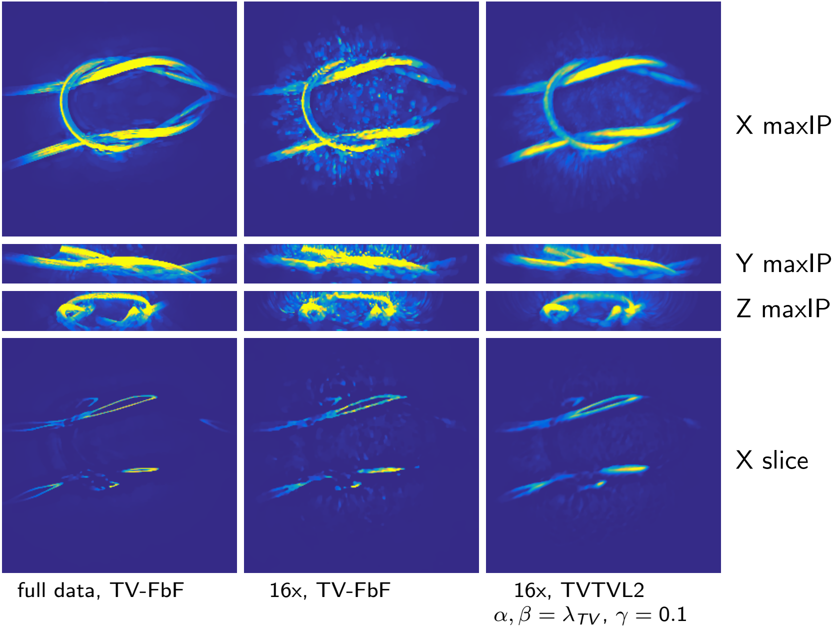

$192 \times 190 \times 108$ voxels, 40 frames

sub-average over 8 frames

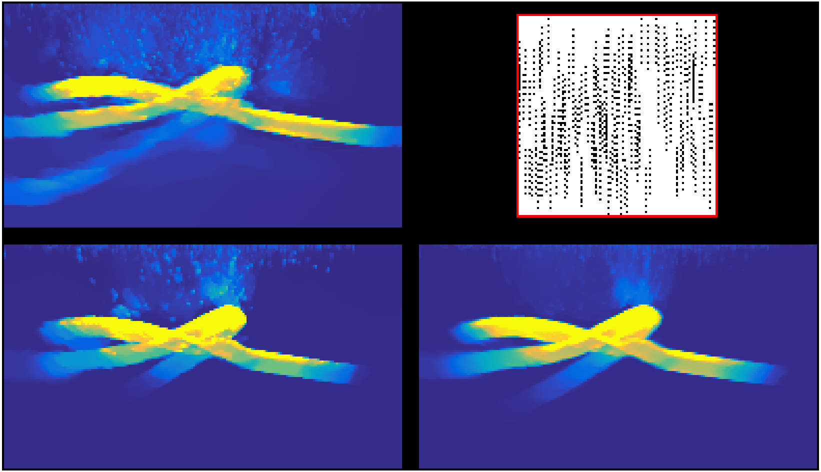

TV-FbF

TVTVL2, $\alpha = \beta = \lambda_{TV}$, $\gamma = 0.1$

Photoacoustic Tomography

- Imaging with laser-generated ultrasound ("hybrid imaging")
- High contrast for light-absorbing structures in soft tissue.

Challenges of fast, high resolution 4D PAT:

- Nyquist requires several thousand detection points $\rightsquigarrow$ slow.
- High computational load.

Acceleration through sub-sampling:

- Exploit low spatio-temporal complexity to beat Nyquist.
- Acceleration by sub-sampling the incident wave field to maximize non-redundancy of data.
- Adjoint PAT operator allows to use variational/iterative approaches.
- Sparse variational regularization gives promising results.

- **Arridge, Beard, Betcke, Cox, Huynh, L, Zhang, 2017**. *Enhancing Compressed Sensing Photoacoustic Tomography by Simultaneous Motion Estimation*, *in preparation.*

- **Arridge, Beard, Betcke, Cox, Huynh, L, Ogunlade, Zhang, 2016**. *Accelerated High-Resolution Photoacoustic Tomography via Compressed Sensing*, *Physics in Medicine and Biology* 61(24).

- **Arridge, Betcke, Cox, L, Treeby, 2016**. *On the Adjoint Operator in Photoacoustic Tomography*, *Inverse Problems* 32(11).

cmic Centre for Medical Image Computing

k-Wave

EPSRC Engineering and Physical Sciences Research Council

NVIDIA.

We gratefully acknowledge the support of NVIDIA Corporation with the donation of the Tesla K40 GPU used for this research.

Thank you for your attention!

- **Arridge, Beard, Betcke, Cox, Huynh, L, Zhang, 2017**. *Enhancing Compressed Sensing Photoacoustic Tomography by Simultaneous Motion Estimation*, *in preparation.*

- **Arridge, Beard, Betcke, Cox, Huynh, L, Ogunlade, Zhang, 2016**. *Accelerated High-Resolution Photoacoustic Tomography via Compressed Sensing*, *Physics in Medicine and Biology* 61(24).

- **Arridge, Betcke, Cox, L, Treeby, 2016**. *On the Adjoint Operator in Photoacoustic Tomography*, *Inverse Problems* 32(11).

cmic Centre for Medical Image Computing

EPSRC Engineering and Physical Sciences Research Council

NVIDIA

We gratefully acknowledge the support of NVIDIA Corporation with the donation of the Tesla K40 GPU used for this research.